

## Effect of High Temperature on Wear Behavior of Stir Cast Aluminium/Boron Carbide Composites

X. CANUTE and M. C. MAJUMDER

*Department of Mechanical Engineering, National Institute of Technology, Durgapur, India*

Received (9 May 2018)

Revised (11 December 2018)

Accepted (20 December 2018)

The need for development of high temperature wear resistant composite materials with superior mechanical properties and tribological properties is increasing significantly. The high temperature wear properties of aluminium boron carbide composites was evaluated in this investigation. The effect of load, sliding velocity, temperature and reinforcement percentage on wear rate was determined by the pin heating method using pin heating arrangement. The size and structure of base alloy particles change considerably with an increase of boron carbide particles. The wettability and interface bonding between the matrix and reinforcement enhanced by the addition of potassium fluotitanate. ANOVA technique was used to study the effect of input parameters on wear rate. The investigation reveals that the load had higher significance than sliding velocity, temperature and weight fraction. The pin surface was studied with a high-resolution scanning electron microscope. Regression analysis revealed an extensive association between control parameters and response. The developed composites can be used in the production of automobile parts requiring high wear, frictional and thermal resistance.

*Keywords:* PCM, enhancement melting, eccentric cylinders, fins, LHS.

### 1. Introduction

Metal matrix composites are widely preferred due to yield strength and wear resistance for high temperature applications [1]. The technology and cost of metal matrix composites depend on manufacturing methods [2]. The mechanical, metallurgical and tribological properties of hybrid metal matrix composites (HMMC) were superior than the aluminium cast metal [3,4]. Aluminium matrix composites possess excellent toughness of a matrix and the strength of reinforcements [5]. Al-B<sub>4</sub>C composites were used in the production of neutron absorber and armour plates, which offer good strength and wear resistance [6]. It is also used in the manufacture of brake drum and rotors. These composites have good fatigue strength and wear resistance in addition to possessing strength, ductility, toughness, thermal and chemical stability and retain mechanical properties at high temperatures [7].

Boron carbide is a prospective reinforcement compared to silicon carbide and aluminium oxide because of its low density, high hardness and thermal stability [8]. Boron carbide has high capability of absorbing neutron and used for manufacturing neutron shielding parts [9].

The combined methodology involving compo casting and squeeze casting yield a better casting with less porosity [10]. Lashgari et al. [11] investigated the impact of strontium in aluminium boron carbide stir cast composites. They proved that adding strontium to aluminium boron carbide composites increased wear resistance. The addition of boron carbide to Aluminium alloy matrix yield improved mechanical properties and boron carbide particles were uniformly distributed in the aluminium matrix. Kalaiselvan et al. [12] investigated the influence of boron carbide particles (20  $\mu\text{m}$ ) with different compositions (2%, 4%, 6% and 8%) in A359 alloy matrix. The experimental results revealed that the A359/B<sub>4</sub>C/8p composites possessed higher hardness and tensile strength.

Inhomogeneous distribution of particle and porosity are the major difficulties in producing Al/B<sub>4</sub>C composites. The main cause of inhomogeneous distribution is due to low wettability of the boron carbide particles with the aluminium matrix. These problems reduced by controlling process parameters and proper design of the stirrer [13]. Potassium fluotitanate (K<sub>2</sub>TiF<sub>6</sub>) can be added as a flux to promote wettability. It forms a reaction layer of titanium carbide and titanium diboride at the interface [14]. Boron carbide particles were heat treated or coated to improve wettability.

The tribological behaviour of the material depends on the morphological content of the composites and operating conditions like load, speed, temperature, environment and counter body material [15]. The wear resistance at high temperature is affected by the yield strength and toughness of material [16].

The methods available for high-temperature pin on disk tests are chamber heating and pin heating method. Pin heating method is preferred because high temperatures are reached within a short period. The effect of load, sliding speed and temperature on the wear of stainless steel was studied earlier. The frictional coefficient and surface finish increase with temperature. The wear fragments produced during the wear act as hard material which gradually transforms the two body abrasive mechanism into three body abrasive mechanism. This phenomenon leads to more material loss at elevated temperatures [17]. Radhika et al. [18] studied the effect of load, sliding speed and sliding distance of Al-Al<sub>2</sub>O<sub>3</sub>/9p-Gr/3p composites was investigated earlier and concluded that sliding distance significant effect when compared to other parameters. The bulk temperature of the pin is greater than the disc and the wear rate of the stationary pin on the steel disc. Selvakumar et al. [19] conducted wear studies on 6Al-4V-B<sub>4</sub>C composites and concluded that the wear resistance increased with a rise in the nano-boron carbide particulate content. The predominant wear mechanisms in the tribological behaviour are abrasion, oxidation and delamination.

Kumar et al. [20] investigated the influence of temperature and load on the wear behaviour aluminium alloy-titanium diboride composites and concluded that the wear rate decreases with a rise in temperature and content of titanium boride particles. Panwar et al. [21] studied the wear behaviour of aluminium zircon composites with varying particle size by stirring casting method. They concluded that volume

loss of the composites increased with load and temperature. The wear rate of fine particle composites was higher than the coarse grain size reinforced composites. The wear parameters load and temperature played a significant role on wear rate than sliding velocity in the investigation of tribological behaviour on aluminium silicon carbide composites [22]. The wear rate decreases with a rise in the reinforcement content in the tribological study of Al6063/TiB<sub>2</sub> composites [23]. The wear behavior is affected mostly by the temperature applied. The wear resistance decreased when the temperature is increased. High metal flow was observed at high temperature [24]. Kumar et al. [25] studied the influence of reinforcements of zircon sand and silicon particles in aluminium LM13 alloy and found the wear rate increases with an increase in temperature. The increase in wear rate is due to the removal of oxide layer during sliding action between pin and steel disc.

The current investigation was focussed on the evaluation of high temperature wear behaviour of Al-B<sub>4</sub>C composites with different weight fractions of boron carbide.

## **2. Material and methods**

### **2.1. Materials**

Aluminum A356 possess good castability, corrosion resistance, machinability and weldability. Aluminium alloy A356 is a silicon-magnesium alloy with 0.2% iron and 0.1% zinc. Aluminium alloy has a greater elongation, higher strength. The important applications It has good thermal stability, corrosion resistance, ductility, strength and elongation. Aluminium A356 alloy is mixed with boron carbide powder (4%) by the stir casting method. Boron carbide powder (63 microns) used as the primary reinforcement material. Magnesium powder was added to increase strength and reduce casting fluidity and surface tension in aluminum.

### **2.2. Stir Casting**

Boron carbide powder is heated to 750°C for three hours and added in the melt. The calculated amount of aluminium cast metal was charged into the stir-casting furnace and the temperature was increased to 850°C. The temperature was decreased progressively reaches to semisolid state.

Hexachloroethane tablets were added to melt to remove the entrapped air and porosity. The preheated boron carbide particles were added in the liquid melt. Potassium fluotitanate powder, aluminium-strontium master alloy and magnesium were added in required proportions. The slurry is heated to full liquid state and temperature upheld at 750°C. The melt was agitated continuously for 15 minutes. The pouring temperature was maintained at 720°C.

### **2.3. Microstructural characterization**

The material characterization was carried out by using microstructure and SEM analysis. The composite specimens for material characterization made with dimensions of 13 mm diameter and 25 mm length. The sample preparation consisted of polishing with emery paper from 600 to 1200 grit size, Al<sub>2</sub>O<sub>3</sub> suspension and diamond paste. The polished sample was etched with keller reagent and examined through the optical microscope (NIKON Epiphot 200) with magnifications like

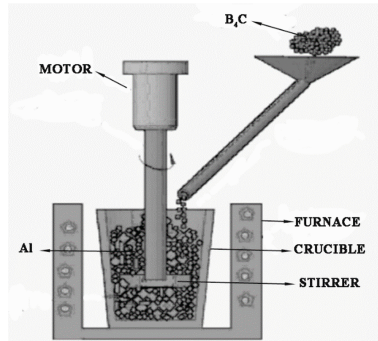


**Figure 1** Schematic diagram of stir casting setup

100X, 200X and 500X. SEM micrographs were taken by the scanning electron microscope (Model: SIGMA Carl Zeiss Microscopy Ltd, UK) at various magnifications with energy dispersive (EDX) detector.

#### 2.4. Mechanical tests

The tensile strength was determined using the universal material tester. The dimensions of the tensile test specimen according to ASTM E8 standards. The specimen has a diameter of 10 mm diameter with a length of 75 mm. The specimen tested at a crosshead speed of 1 mm/min. The hardness test was carried out with a micro-hardness tester (Model: Mitutoyo MVKH1) having features like automatic load control and an accuracy of  $\pm 1\%$ . The experiment carried out under load of 50g with a dwell time of 20 seconds.



**Figure 2** POD wear and friction apparatus

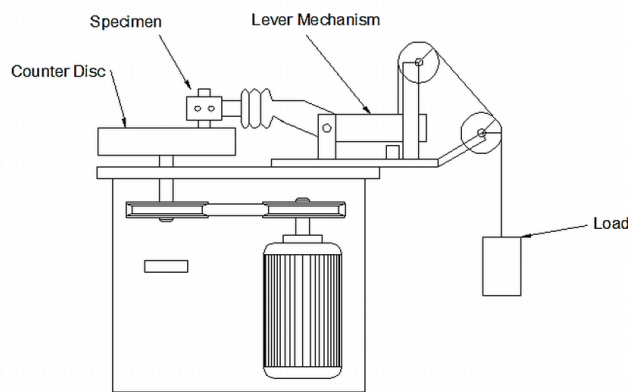


**Figure 3** Schematic diagram

Wear tests of Al-B<sub>4</sub>C composites were performed by POD machine (DUCOM). Schematic diagram and photograph of POD Wear and Friction apparatus are shown in Fig. 2 and Fig. 3 respectively. Fig. 4 illustrates the pin heating arrangement. The dimensions of the steel disc material measured  $\Phi 165 \times 8$  mm thick. The surface roughness of the steel disc is  $0.5 \mu\text{m}$ . The specimens were tested in non-abrasive and dry sliding conditions. The specimen was lapped by 1200 grit paper. Initial and final weight was noted by a digital electronic balance (Model: SHIMADZU AUY 220) with an accuracy of 0.1 mg. The pin is inserted in the collet which is surrounded by heater coil. The pin is held pressed against EN 32 steel disc. The wear tests were conducted at load of 10, 20 and 30 N, sliding velocity of 1, 2 and 3 m/s and varied weight fraction of the reinforcement. Track diameter of disc of 110 mm was used for the entire test.

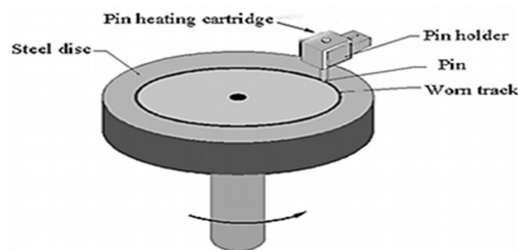


**Figure 4** Pin heating arrangement

### 3. Plan of experiments

The experimental plan was designed considering taguchi principles and DOE. The parameters considered were load, sliding velocity, temperature and reinforcement

content for this work. The experimental conditions levels and parameters are shown in Table 1.

**Table 1** Experimental conditions

Level	A Load [N]	B sliding velocity [m/s]	C Temperature [°C]	D Weight fraction [%]
1	10	1	60	4
2	20	2	120	8
3	30	3	180	12

**Table 2** Experimental values

Trial No.	Load A	Sliding velocity B	Temperature C	Weight fraction D	Wear rate WR	S/N ratio
1	10	1	60	4	0.001651	55.6451
2	10	2	120	8	0.001852	54.6472
3	10	3	180	12	0.001573	56.0654
4	20	1	120	12	0.002272	52.8718
5	20	2	180	4	0.002621	51.6307
6	20	3	60	8	0.001623	55.7936
7	30	1	180	8	0.005530	45.1455
8	30	2	60	12	0.003587	48.9054
9	30	3	120	4	0.003102	50.1672

The orthogonal array used for the study is L9. The choice of an array was based on the condition that the degrees of freedom should be greater than or equal to the sum of the variables [26]. The experimental values were analyzed by ANOVA method. Wear rate was examined as the response variable. The data analysis was carried through MINTAB 16 software. The experimental data were converted to signal to noise ratio.

The details of the results of the various mechanical, metallurgical and tribological tests are presented in this section.

## 4. Results and discussion

### 4.1. Microstructure analysis

The microstructure of aluminium cast alloy and Al/B<sub>4</sub>C composites with different proportions of boron carbide are shown in the Figs. 5 to 8. The boron carbide and zirconium oxide particles distributed evenly in the aluminium matrix.

The microstructure shows the fine equiaxed structure of  $\alpha$ -aluminum dendrites and reinforcement particles are bonded to the matrix alloy. The small  $\alpha$ -aluminum grains are evenly distributed between grain boundaries. The phases like Mg<sub>2</sub>Si and CuAl<sub>2</sub> dispersed in the matrix contribute to alloy strengthening.

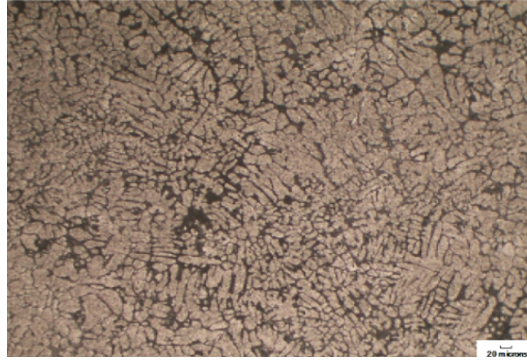


**Figure 5** Microstructure of Al A356(100X)

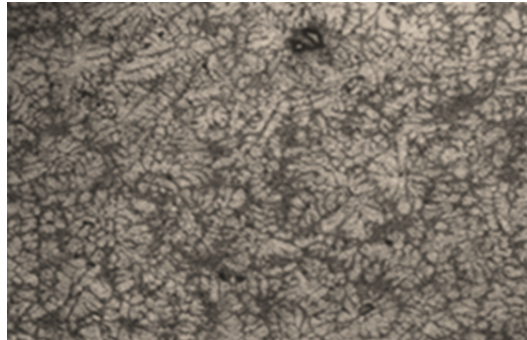


**Figure 6** Microstructure of Al/4B<sub>4</sub>C composite (100X)

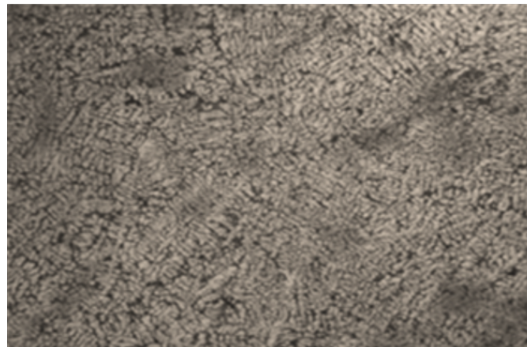


**Figure 7** Microstructure of Al/8B<sub>4</sub>C/3Gr composite (100X)

#### 4.2. SEM investigation

The SEM images shown in Figs. 9 to 11. The SEM images show the uniform distribution of reinforcement particles in the matrix and formation of the reaction layer (TiB<sub>2</sub> and TiC) on boron carbide particle surface [14]. The homogenous reinforcement particle distribution improve the mechanical properties like hardness,

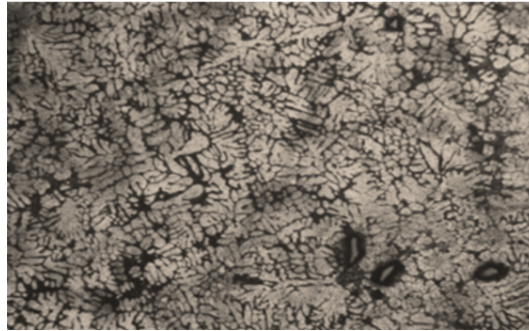


**Figure 8** Microstructure of Al/12B<sub>4</sub>C (100X)

tensile and impact strength. With the addition of potassium fluotitanate ( $K_2TiF_6$ ), bonding of reinforcement particles with aluminium matrix is effective. The silicon particles modified from acicular to fine fibrous structure by the addition of strontium were the subject of earlier analyses. The transient layer is formed between the reinforcement particles and matrix due to the modification of matrix alloy.

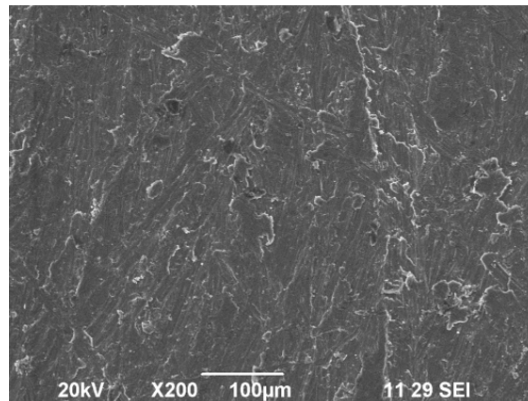


**Figure 9** SEM image of Al/4B<sub>4</sub>C composite(200X)

#### 4.3. Wear test results

The readings of the wear test were recorded and results of wear analysis calculation are tabulated (Tab. 2). The upshot of the load, speed and temperature on the wear rate was analysed by MINITAB 16 software.

#### 4.4. Effect of process parameters on response

The parameter with the highest S/N ratio gives minimum wear rate. The optimum wear rate is observed at load 10N with sliding velocity 3m/s, temperature 60°C and weight fraction 12%. Response values for S/N ratio are shown in Tab. 3 and means in Tab. 4. The main effects plot for S/N ratio is shown in Fig. 12.



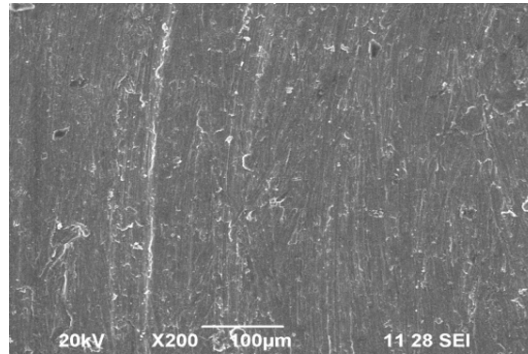


**Figure 10** SEM image of Al/8B4C composite(200X)

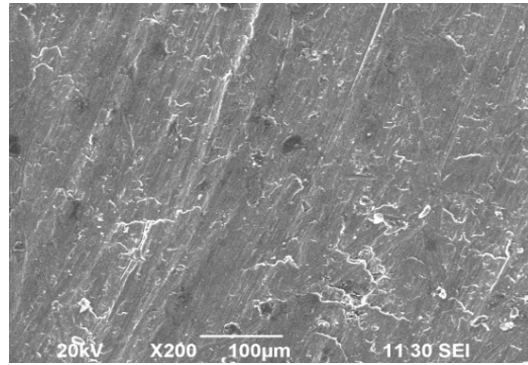


**Figure 11** SEM image of Al/12B4C composite(200X)

**Table 3** Response table for signal to noise ratio

Level	Load	Sliding velocity	Temperature	Weight fraction
1	55.45	51.22	53.45	52.48
2	53.43	51.73	52.56	51.86
3	48.07	54.01	50.95	52.61
Delta	7.38	2.79	2.50	0.75
Rank	1	2	3	4

**Table 4** Response table for means

Level	Load	Sliding velocity	Temperature	Weight fraction
1	0.001692	0.003151	0.002287	0.002458
2	0.002172	0.002687	0.002409	0.003002
3	0.004073	0.002099	0.003241	0.002477
Delta	0.002381	0.001052	0.000954	0.0005444
Rank	1	2	3	4

The main effect of plots for means is shown in Fig. 13. Load has significant impact on wear compared to sliding velocity, temperature and weight fraction. From the main effects plot for means, wear rate increases with load. When sliding velocity

is increased the contact time between the disc and the pin decreases. Hence the wear rate is decreased. From the response table for S/N ratios it is inferred that the load has the significant effect on wear rate, followed by sliding speed, temperature and weight fraction.

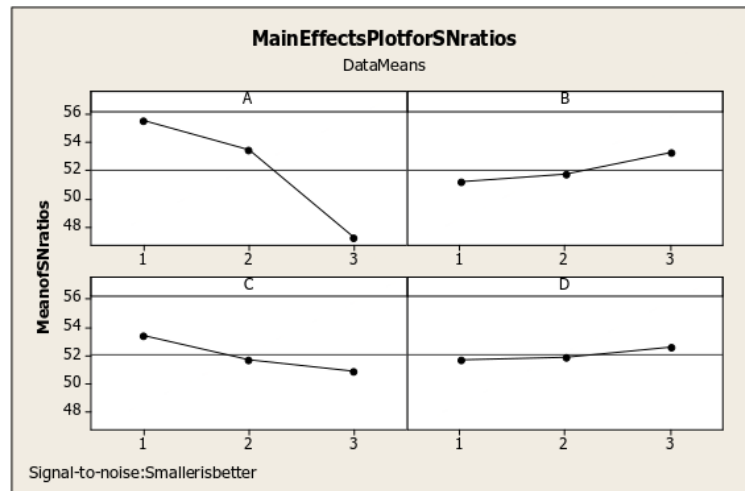


Figure 12 Main effects plot for signal to noise ratio

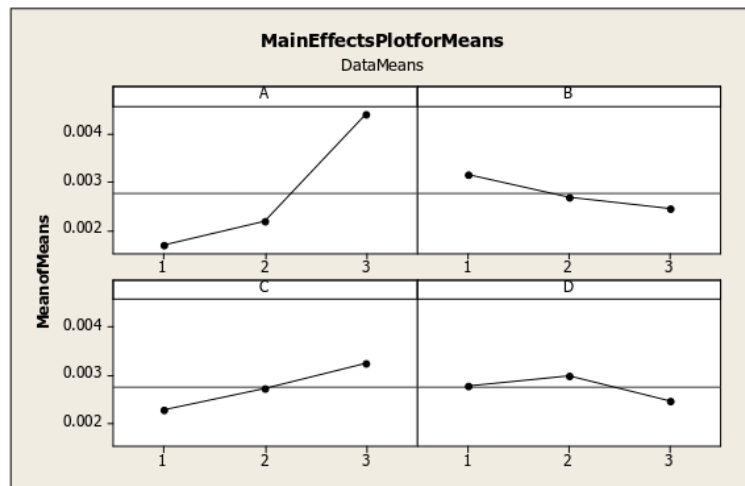


Figure 13 Main effects plot for means

Wear rate advances with applied load. Wear rate increase with the rise in temperature due to softening of the material. Wear rate decreases when the sliding velocity is increased from 2 to 3m/s. Abrasive wear increases with an increase in temperature. Hardness, flow stress and yield strength decrease when temperature

**Table 5** ANOVA for wear rate

Source	DF	SS	Adj. MS	F	P [%]
Load, A	2	0.0000085	0.00000425	121.9512	63.57659484
Sliding Velocity, B	2	0.0000018	0.0000009	25.82496	13.46327891
Temperature, C	2	0.000002	0.000001	28.6944	14.95919879
Weight fraction, D	2	0.000001	0.0000005	14.3472	7.479599393
Pooled Error	2	6.97E-08	3.485E-08		0.521328078
Total	8	1.34E-05	1.67121E-06		100

increases [27]. ANOVA analysis was performed with a 95% confidence level and 5% significance level (Tab. 5). The applied load has the greater statistical influence 63.58% and followed by temperature 14.96%, sliding velocity 13.46% and weight fraction 7.48. The values of regression coefficient  $R^2$  for wear rate is 87.93%.

#### 4.5. Multiple regression analysis

A regression equation was generated by the correlation of process parameters like load, sliding velocity and temperature. Regression equation establishes the equation between the parameters like load, sliding velocity and temperature and weight fraction.

$$WR = 0.00034 + 0.00119 \times A - 0.000526 \times B + 0.000477 \times C + 0.000010 \times D$$

The regression equation predicts the wear rate for aluminium boron carbide composites. From the above relation, it was observed that the coefficient associated with load, temperature and weight fraction was positive. This clearly reveals that as load, temperature and weight fraction increases, the wear rate of the hybrid composite also increases. The negative coefficient of sliding velocity reveals that an increase in sliding velocity decreases the wear rate. The friction coefficient decreases with the increase in the content of the boron carbide particles. The boron carbide particles form a protective layer between the surface of pin and counterface material [28]. The wear rate is higher for unreinforced alloy for levels of temperature. The wear rate increases with increase in the temperature for particular weight of boron carbide particles. The contact area between pin and steel increases with the increase in temperature [29].

#### 4.6. Analysis of worn pin surface

Detailed scanning electron microscope analysis of the worn pin surfaces is shown by Figs. 14–16. Fine and shallow grooves formed at low applied load and speed due to abrasive wear. The particles of the steel disc penetrate into the pin and hence wear on the pin is accelerated. Hard boron carbide particles remove more material from the worn surface at higher load. The phenomenon is due to delamination. Due to softening of the material, extra material is removed from pin at high temperature [30]. Delamination wear is more at higher temperature. The phenomenon of adhesive wear is predominant at maximum load 30 N. Wear tracks vanish at this juncture. Boron carbide particles tend to gather at the boundaries of  $\alpha$ -aluminium dendrites [31].

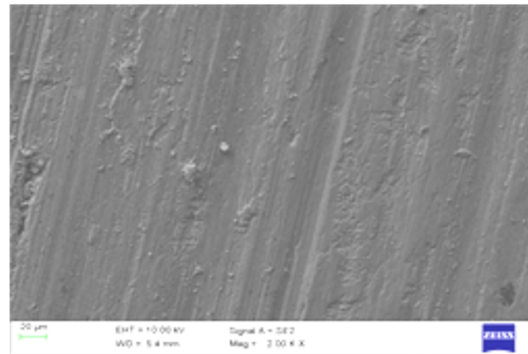


**Figure 14** SEM image ( $L=10\text{N}$ ,  $S=2\text{m/s}$ ,  $T=120^\circ\text{C}$ ,  $W=8\%$ )

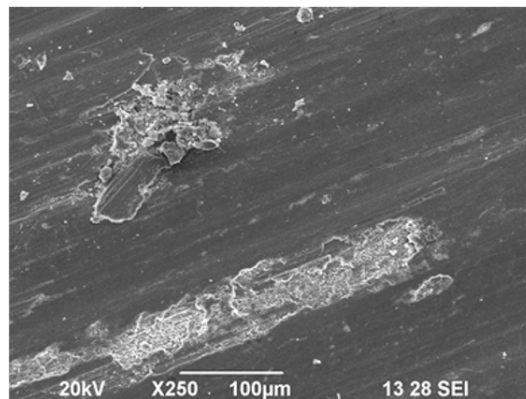


**Figure 15** SEM image ( $L=20\text{N}$ ,  $S=2\text{m/s}$ ,  $T=180^\circ\text{C}$ ,  $W=4\%$ )

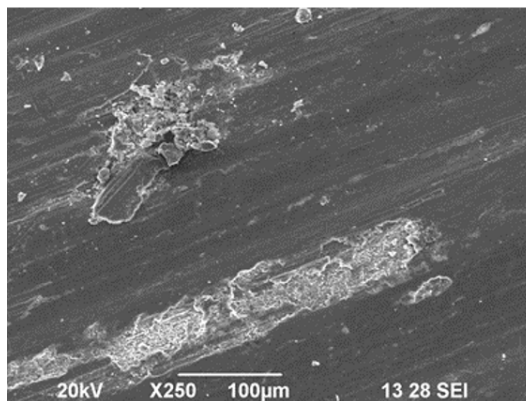


**Figure 16** SEM image ( $L=30\text{N}$ ,  $S=2\text{m/s}$ ,  $T=60^\circ\text{C}$ ,  $W=12\%$ )

SEM image of the worn out pin surface at  $L=30\text{N}$ ,  $S=3\text{ m/s}$ ,  $T=120^\circ\text{C}$ ,  $W=4\%$ ) is shown in Fig. 17. The grooves widen with increased load. EDS image (Fig. 18)

reveals carbon, iron, silicon, boron, silicon, magnesium and aluminium. Mixed mechanical layer exhibits extreme hardness. The amount of wear debris formed is higher at increased load. Also the width of the grooves is also larger [32]. The mechanism of wear rate is greatly affected by the two sliding surface interaction.

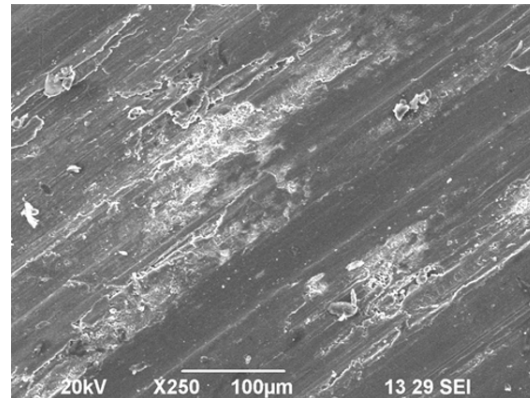


**Figure 17** SEM image (L=30N S=3 m/s T=120° C, W=4%)

The heat due to friction between the surface of the pin and disc is increased by the load and duration of the test [33]. Wear rate of the composites augmented linearly with increasing the temperature at high load. This effect is due to the formation of the oxide film and glazing layer on sliding components. These layers prevent the direct metal-to-metal contact of sliding surfaces during sliding. Deeper ploughing marks were observed at higher temperature and craters were formed. This phenomenon significantly increases the wear rate. The addition of strontium based master alloy converts large  $\alpha$  aluminium grains to fine equiaxed grains and eutectic silicon plates into fine particles. This phenomenon increases the mechanical properties and wear resistance.

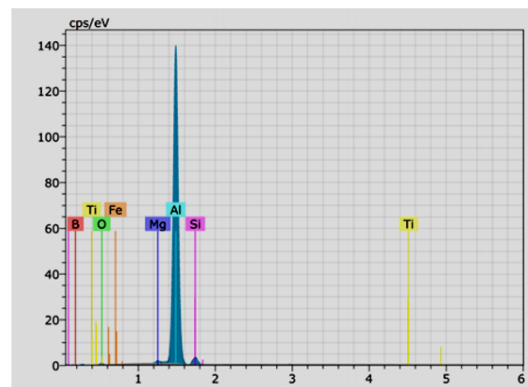


**Figure 18** EDS image spectra of (L=20N S=3 m/s T=60°C)

#### 4.7. Confirmation test

The confirmation tests were conducted with optimum parameters arrived by MSEXCEL solver (Tab. 6). The error found to be less than 5%. The error between predicted and test value is 2.433%.

**Table 6** Results of confirmation experiments

Parameter Parameter	Optimal conditions Excel Solver	Predicted value	Experimental value
Wear Rate	A1, B3, C1,D3 (30 N, 1 m/s, 60° C, 12 %)	0.0004411	0.0004521

#### 5. Conclusion

Aluminium boron carbide composites were manufactured by the melt stirring technique. The wear rate of the A356/B<sub>4</sub>C composites increased with the addition of B<sub>4</sub>C particles in A356 alloy matrix. Also the wear rate of the hybrid composite increases with the load and temperature. Increase in sliding velocity decreases the wear rate. The addition of strontium increases the tribological behaviour of the composites.

The wear rate increases with an increase in applied load and temperature and decreases with the increase in sliding velocity. S/N ratio analysis indicates the optimum wear rate is observed at 10N load with sliding velocity 3m/s temperature 60° C and weight fraction, 12%. From the ANOVA analysis, it was found that applied load has the highest significance on wear rate followed by temperature and sliding velocity. The wear rate decreases with an increase in the reinforcement content.

Regression analysis revealed a close relationship between input parameters and response. The confirmation experiment revealed that the error between the experimental values and optimal predicted values were less than 5% and hence the experimental results are validated.

Aluminium boron carbide MMC's have encouraging applications in the manufacture of high temperature resistant parts. The tribological behaviour of Al-B<sub>4</sub>C composites at higher temperature can be enhanced by choosing reduced particle size, and intermetallic material and titanium based master alloys.

#### References

- [1] Myriounis, D.P., Hasan, S.T. and Matikas, T. E.: Micro deformation behaviour of Al-SiC 17 Metal Matrix Composites, *Composite Interfaces*, **15**(5), 485–514, **2008**.
- [2] Deborah, D.L: *Composite Materials, Science and Applications*, Second Edition, London: Springer-Verlag Limited, **2010**.
- [3] Shanta, S., Krishna, M., Jayagopal, U.: A study on damping behaviour of aluminate particulate reinforced ZA-27 alloy metal matrix composites, *Journal of Alloys and Compounds*, **314**, 268–274, **2001**.
- [4] Michael, O.B., Kenneth, K., Alaneme, L., Heath, C.: Aluminium matrix hybrid composites: a review of reinforcement philosophies; mechanical, corrosion and

- tribological characteristics, *Journal of Material Research Technology*, **4**(4), 443–445, **2015**.
- [5] **Terry, B. and Jones, G.**: *Metal Matrix Composites – current developments and future trends in industrial research and applications*, Oxford: Elsevier Advanced Technology, **1990**.
- [6] **Kainer, K.U.**: *Metal matrix composite custom made material for automotive and aerospace engineering*, Weinheim: Wiley VCH Verlag GmbH & Co KGaA, **2006**.
- [7] **Pyrzik, A.J., Newman, R.A. and Allen, S.**: High temperature strength retention of aluminum boron carbide (AlBC) composites, in: *Proceedings of 31 st International conference on advanced ceramics and composites at Daytona Beach, FL*, The American Ceramic Society, **2007**.
- [8] **Jung J., Kang, S.**: Advances in manufacturing boron carbide-aluminium composites, *Journal of American Ceramic Society*, **87**(1), 47–54, **2004**.
- [9] **Khakbiz M., Akhlagi, F.**: Synthesis and structural characterization of Al-B<sub>4</sub>C nano-composite powder by mechanical alloying, *Journal of Alloys and Compounds*, **479**, 334–341, **2009**.
- [10] **Rajan, T.P.D., Pillai, R.M., Pai, B.C., Satyanarayana, K.G., Rohatgi, P.K.**: Fabrication and characterization of Al-7Si-0.35Mg/flyash metal matrix composites processed by different stir casting routes, *Composites Science and Technology*, **67**, 3369–3377, **2007**.
- [11] **Lashgari, H.R., Emamy, H.R.M., Razaghian, A. and Najimi, A.A.**: The effect of strontium on microstructure, porosity and tensile properties of A356-10% B<sub>4</sub>C cast composites, *Material Science and Engineering*, **517**(1), 170–179, **2009**.
- [12] **Kalaiselvan, K., Murugan, N., Parameswaran, S.**: Production and Characterization of Al 6061-B<sub>4</sub>C stir composite, *Material Design*, **32**(7), 4004–4009, **2011**.
- [13] **Harun, M.B., Shamsudin, S.R., Yazid, H., Selamat, Z., Sattar, M.S., Jalil, M.**: Microstructure Porosity and Hardness in Al-(Si-Mg) Cast composites, *ASEAN Journal for Science and Technology Development*, **23**(1&2), 113–122, **2006**.
- [14] **Toptan, F., Kilcarselan, A.**: Processing and microstructural characterization of AA1070 and AA6063 matrix B<sub>4</sub>Cp reinforced composites, *Materials and Design*, **31**, S87–S90, **2010**.
- [15] **Dwivedi, D.K., Sharma, A., Rajan, T.V.**: Interface temperature under dry sliding conditions, *Materials Transactions, Japan Institute of Metals*, **43**(9), 2256–2261, **2002**.
- [16] **Sundstorm, A., Rendon, J., Olsson, M.**: Wear behaviour of some low alloyed steels under combined impact/abrasion contact conditions, *Wear*, **250**, 744–754, **2001**.
- [17] **Parathasarathi, N.L., Borah and Alber, K.**: Correlation between coefficient of friction and surface roughness in dry sliding wear of AISI 316L(N) stainless steel at elevated temperatures, *Computer Modelling and New Technologies*, **17**(1), 51–63, **2013**.
- [18] **Radhika N., Subramanian R., Venkat Prasat, S.**: Tribological behaviour of Aluminium/Alumina/Graphite Hybrid Metal Matrix Composite using Taguchi's Techniques, *Journal of Minerals & Materials Characterization & Engineering*, **10**(5), 427–443, **2011**.
- [19] **Selvakumar, N., Ramkumar, T.**: Effects of High Temperature Wear Behaviour of Sintered Ti-6Al-4V Reinforced with Nano B<sub>4</sub>C Particle, *Transactions of the Indian Institute of Metals*, 223–231, **2016**.

- [20] **Kumar, S., Subramanya Sarma, V., Murty, B.:** Effect of Temperature on the Wear Behavior of Al-7Si-TiB<sub>2</sub> In-Situ Composites, *Metallurgical and Materials Transaction A*, **40**(1), 223–231, **2009**.
- [21] **Panwar, R.S., Pandey, O.P.:** Analysis of wear track and debris of stir cast LM13/Zr composite at elevated temperatures, *Materials Characterization*, **75**, 200–213, **2013**.
- [22] **Shanmughasundaram, P.:** Effect of Temperature, Load and Sliding Velocity on the Wear Behavior of AA7075–SiC Composites, *Mechanics and Mechanical Engineering*, **21**(1), 85–93, **2017**.
- [23] **Natarajan, S., Narayanasamy, R., Kumaresh Babu, S.P., Dinesh, G., Anil Kumar, B., Sivaprasad, K.:** Sliding wear behaviour of Al6063/TiB<sub>2</sub> in situ composites at elevated temperature, *Materials and Design*, **30**(7), 2521–2531, **2009**.
- [24] **Michael Rajan, H.B., Ramabalan, S., Dinaharan, I., Vijay, S.J.:** Effect of TiB<sub>2</sub> content and temperature on sliding wear behavior of AA7075/TiB<sub>2</sub> in situ aluminum cast composite, *Archives of Civil and Mechanical Engineering*, **14**, 72–79, **2014**.
- [25] **Kumar, S., Panwar, R.S. and Pandey, O.P.:** Effect of dual reinforced ceramic particles on high temperature tribological properties of aluminium composites, *Ceramics International*, **39**, 6333–6342, **2013**.
- [26] **Roy, K.R.:** *A Primer on the Taguchi Method*, Van Nostrand Reinhold, NewYork, NY. **1990**.
- [27] **Lindroos, M., Apostol, V., Heino, K., Valtonen, K., Laukkanen, A., Holmberg, K. and Kuokkala, V.T.:** The deformation, strain hardening, and wear behavior of chromium-alloyed hadfield steel in abrasive and impact conditions, *Tribology Letters*, **57**(3), 1–17, **2015**.
- [28] **Stott, F.:** High temperature sliding wear of metals, *Tribology International*, **35**(8), 489–495. **2002**.
- [29] **Selvakumar, N., Ramkumar, T.:** Effects of High Temperature Wear Behaviour of Sintered Ti–6Al–4V Reinforced with Nano B<sub>4</sub>C Particle, *Transactions of the Indian Institute of Metals*, **69**(2), 223–231, **2016**.
- [30] **Radhika, N., Vaishnavi, A. and Chandran, G.K.:** Optimisation of Dry sliding wear process parameters for Aluminium Hybrid Matrix composites, *Tribology in Industry*, **36**(2), 188–190, **2014**.
- [31] **Rohatgi, P.K., Guo, R.Q.:** Low Cost Cast Aluminium–Fly Ash Composites for Ultralight Automotive Application, *TMS Annual Meeting, Automotive Alloys*, 157–168, **1997**.
- [32] **Radhika, N., Balaji, T., Palaniappan, S.:** Studies on mechanical properties and tribological behaviour of LM25/SiC/Al<sub>2</sub>O<sub>3</sub>, *Journal of Engineering Science and Technology*, **10**(2), 134–144, **2015**.
- [33] **Dixit, G., Khan, M.M.:** Sliding Wear Response of an Aluminium Metal Matrix Composite: Effect of Solid Lubricant Particle Size, *Jordan Journal of Mechanical and Industrial Engineering*, **8**(6), 351–358, **2014**.